Surface-enhanced Raman scattering: facts and inline trends

Mohammad Kamal Hossain and Yukihiro Ozaki*

Department of Chemistry, School of Science and Technology, Kwansei Gakuin University, Gakuen 2-1, Sanda, Hyogo 669-1337, Japan

Raman spectroscopy is a complete and comprehensive analytical tool that can be used to make a bridge between industrial interests and the 'Terabithia' world. Surface-enhanced Raman scattering (SERS), a subset of Raman spectroscopy, exhibits greater potential over other complementary techniques. Further, tip-enhanced Raman scattering and plasmon excitations ranging from the visible to the near-infrared region using nanostructured materials have unprecedented scope in different sectors related to SERS. In this review, an attempt has been made to trace the progress of surface-enhanced Raman spectroscopy and its potential in different multidisciplinary studies. Starting from key terminologies in brief, several applications are pointed.

Keywords: Imaging, metal nanoparticles, surface-enhanced Raman scattering, surface plasmon resonance.

Introduction

RAMAN spectroscopy deals with a change in frequency when light is scattered by molecules or atoms adsorbed on the substrate[1]. Hence, it provides the molecular identity or fingerprint, information on molecular structure, intermolecular interaction and inherent dynamics[2–5]. It is a non-destructive and non-invasive technique, including *in situ* and *in vitro* analysis of biological samples. Raman spectroscopy can be carried out under a wide range of conditions, viz. temperature, pressure, etc.[6,7]. Despite all these benefits, Raman scattering is inefficient and is not often used for practical applications because of its low cross-section, ~10^{-30} cm^2, nearly 15 orders of magnitude lower than complementary fluorescence excitation.

Although intense Raman scattering was reported by Fleischmann *et al.*[8] without any indication of surface-enhanced Raman scattering (SERS), Jeanmaire and Van Duyne[9], and Albrecht and Creighton[10] pointed out the influence of a roughened surface on the unusually high Raman intensity (thereafter was known as SERS). This was an immediate breakthrough for using Raman scattering in science and technology to overcome the low cross-section signal quality inherent in pre-SERS Raman spectroscopy. This technique has attracted more attention due to its greater signal enhancement compared to the normal Raman spectroscopic method. The application of SERS in surface analysis, catalysis, forensic science, biotechnology, homeland security, and other disciplines, is drawing interests because of the irreplaceable benefits of this technique[11–15]. In this article, we have attempted to elaborate the facts and inline trends of SERS in science and technology. After a brief description about SERS itself, including the mechanisms behind it, several typical potential applications of this technique have been outlined.

*For correspondence. (e-mail: ozaki@kwansei.ac.jp)

The story behind SERS

SERS is a particular subset within the realm of Raman spectroscopy, where for certain molecules adsorbed on a specially prepared metal surface, a Raman spectrum is observed whose intensity exceeds that of the normal Raman spectrum[16,17] by a factor of 10^8–10^{10}. A simplified schematic is shown in Figure 1 *a*. Once the SERS-active substrate is exposed to laser excitation, the analyte adsorbed nearby gets polarized and emits enhanced Raman signal. The phenomenon corresponds to surface plasmon resonance (SPR)-mediated intense electromagnetic (EM) field distribution at the apex or the sharp verges of SERS-active substrates. Figure 1 *b* depicts the

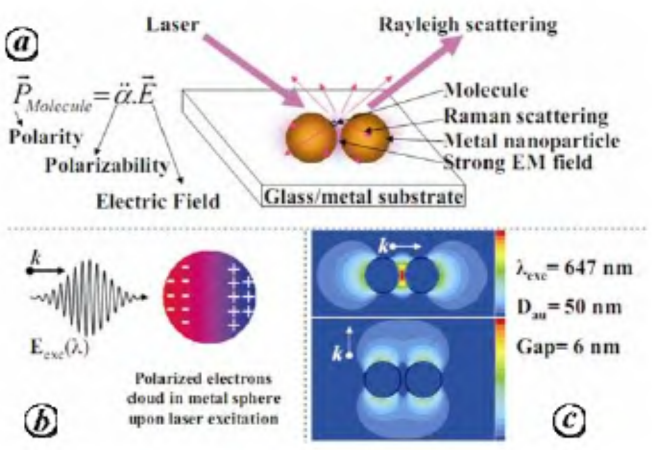

Figure 1. *a*, Simplified schematic of the SERS process. *b*, Polarized electron cloud in a metal sphere upon laser excitation. *c*, Finite-difference time-domain analysis of a metal nanoparticle dimer. Localized EM field distribution occurs only in s-polarization. Colour bar represents 0–20 dBV/m.

distribution of the electron cloud of typical nanoparticles and the oscillation is coherent with that of the incident photons. Using time-variant Maxwell equation, one can easily get the EM field distribution surrounding the nanoparticles. Figure 1 *c* shows that localized EM field distribution occurs only in s-polarization. Thus the analyte existing at the centre of this distribution will experience maximum influence and shows strongest enhancement in SERS.

As was mentioned earlier, in 1977, two groups (i.e. those of Van Duyne and Creighton) independently confirmed the influence of a roughened surface on enhanced Raman scattering, in contrast to the first report by Fleischmann *et al.*[8]. They proposed mechanisms for the observed enhancement, which still constitute the underlying principles for modern theories of SERS. Jeanmaire and Van Duyne[9] proposed an EM effect, while Albrecht and Creighton[10] proposed a charge-transfer (CT) effect. One year later, a detailed surface plasmon resonance model for EM enhancement was explained by Moskovits[18] in 1978 and CT complex model through chemisorption was explained by Otto *et al.*[19]. The unbelievable capability of SERS in terms of single-molecule detection was reported in 1997 by two groups, independently, using different experimental set-ups[20,21]. The details underlying the theory has also been reported by many groups, including Moskovits *et al.*[16], Zhang *et al.*[22] and Xu *et al.*[23].

Surface plasmon resonance

Metal nanoparticles are often assumed to comprise of positive ions surrounded by a 'sea of electrons' (i.e. negative ions) and the amount of surface atoms (i.e. the number of free ions) increases with decreasing particle size[24,25]. This 'sea of electrons' is incoherent in motion, and, if excited by EM radiation, may begin to move about and oscillate, generating strong EM fields and forming what are known as plasmons (Figure 1 *a*)[25]. Like all other oscillating systems, these plasmons have a natural or resonant frequency at which they oscillate best. Thus, if incoming light excites these plasmons into their resonant mode, we can get an appreciable increase in the local EM field surrounding the metal. This is the main principle upon which SERS operates; our target molecule is bound onto a metallic surface, and through plasmonic resonance the local EM field and thus the corresponding Raman signal are enhanced.

Surface plasmon resonance (SPR) is a collective excitation mode of the plasma localized near the surface of the metal[26–28]. They can be produced not only by light (on a smooth surface by attenuated total reflection configuration), but also by electrons (on corrugated surfaces of nanoparticles)[27]. It is usual practice to consider the latter case whenever the scientists talk about SPR or localized SPR (SPR) using nanoparticles. The latter case indeed reveals a series of optical phenomena, such as extraordinary transmission of light, light concentration in self-similar chains of metal nanospheres, energy percolation by hybridizing cascaded, localized EM fields, discovery of superlens, etc.[29–34]. The interaction between surface plasmons and the incident photon is known as surface plasmon polariton, a propagating wave along the surface. However, surface plasmons cannot couple directly to free-space EM radiation of the same energy, because they travel too slowly implying that the associated wave vector is too large to satisfy the conservation of energy and momentum. Fortunately, in low k-vector limit these surface modes couple with the free EM field to yield a polariton-type excitation.

SERS mechanisms

The mechanisms involved in SERS enhancement are still under debate. A number of experiments have demonstrated that different effects may contribute to the observed enhanced Raman signal, and two mechanisms have been proposed so far[16,22,23,35,36]. Since the intensity of Raman scattering is proportional to the square of the induced dipole moment (i.e. $\bar{P} = \alpha \cdot \bar{E}$), any enhancement must come from an enhancement of α (molecular polarizability) or from $\boldsymbol{E}$ (the electric field due to the incident radiation). The enhancement associated with $\boldsymbol{E}$ is known as EM enhancement, and the other, associated with α, is known as chemical enhancement.

Two-fold electromagnetic enhancement

The enormous enhancement factor in the order of 10^8–10^{10} is considered to arise mainly from two-fold EM field enhancement[35–37]. This two-fold EM field enhancement is illustrated in Figure 2. Pettinger[36] reported a quantum-mechanical approach for surface-enhanced optical processes summarizing two-fold enhancements; one, from the incident photon–LSPR interaction and two, from the scattered photon–LSPR interaction. In brief, incident photon

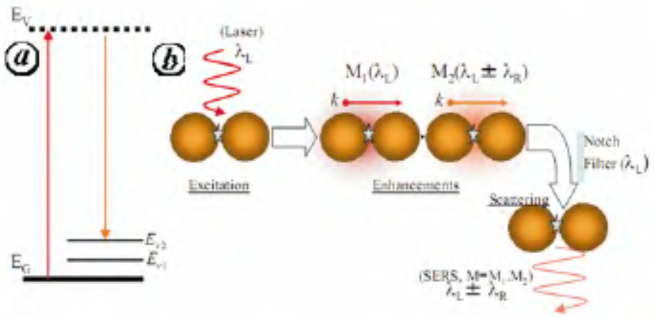

Figure 2. ***a***, Energy-level diagram of the Raman scattering process. ***b***, Schematic diagram of two-fold electromagnetic field enhancement for SERS.

energy irradiated on the adsorbent is scattered from an adsorbate because of LSPR-mediated dipole–dipole interaction (denoted by M_1).

At the same time, the scattered photon from the molecules is in resonance with the plasmon, because its wavelength is close to that of the incident photon. Then the EM field is further enhanced (denoted by M_2) and accumulated strong Raman scattering light is emitted. The enhancement factor for SERS, M, is given by

$$M = \left|\frac{E^{\mathrm{Loc}}(\lambda_{\mathrm{L}})}{E^{\mathrm{I}}(\lambda_{\mathrm{L}})}\right|^2 \times \left|\frac{E^{\mathrm{Loc}}(\lambda_{\mathrm{L}} \pm \lambda_{\mathrm{R}})}{E^{\mathrm{I}}(\lambda_{\mathrm{L}} \pm \lambda_{\mathrm{R}})}\right|^2$$
$$= M_1(\lambda_{\mathrm{L}}) \times M_2(\lambda_{\mathrm{L}} \pm \lambda_{\mathrm{R}}),$$

where E^{I} and E^{Loc} are the amplitudes of the incident and local electronic fields respectively, λ_{L} is the excitation wavelength, $+\lambda_{\mathrm{R}}$ and $-\lambda_{\mathrm{R}}$ are the wavelengths of the anti-Stokes and Stokes Raman shift respectively, and M_1 and M_2 are the first and second enhancement factors respectively.

Chemical effect

In addition to the EM mechanism, several evidences suggest that there is an additional enhancement mechanism which operates independently and both mechanisms can occur simultaneously. In short, a specific interaction of an adsorbate with a nanoparticles surface leads to a charge transfer from the adsorbate into the empty levels on the metal surface or from the occupied surface levels to the adsorbate (Figure 3)[38–41]. Although experimental results have led to a wide acceptance of the order of 10^6 to 10^8 solely due to the EM mechanism, it is also true that

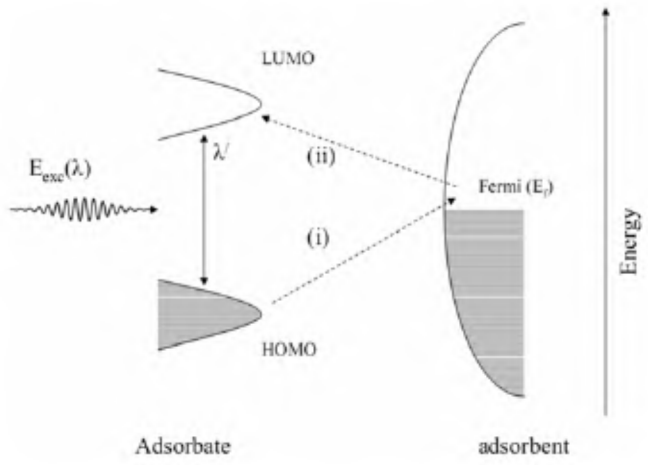

Figure 3. Energy-level diagram of the coupled molecule-adsorbent system. HOMO and LUMO highest occupied and lowest unoccupied molecular orbitals of adsorbates are broadened into resonances by interaction with the metal surface. Possible charge transfer is shown by arrows (i) and (ii). Double-ended arrow shows the possible intermediate resonant Raman process involving molecular states.

the Raman polarizability is substantially enhanced (10 to 1000) when the frequencies of the incident or Raman scattered photons become nearly resonant with the CT excitation of the absorbate–metal coupled system[42,43].

Based on photon–electron couplings, the first complete theory of adsorbate-induced Raman scattering (known thereafter as the CT mechanism) was proposed by Otto's group[44,45]. The idea is to create electron–hole pairs at particular sites and excitations. Once initiated, it interacts strongly with the molecules adsorbed at this site and can be understood by resonant intermediate states in Raman scattering. If a resonant negative state is formed by transformation of an electron between the metal and the adsorbate, the Raman scattering cross-section may be substantially enhanced. The so far well-understood CT mechanism involves the following steps; (a) an incident photon with energy λ induces an intraband transition creating a hole; (b) an electron transfer between the metal and the excited electron level of the adsorbate via tunnelling for physisorbed adsorbates and via hybridizing for chemisorbed adsorbates, and (c) photon emission with energy λ' occurs as this electron recombines with the hole somewhere below the Fermi energy. Since the highest occupied molecular orbit (HOMO) and lowest unoccupied molecular orbit (LUMO) of the adsorbate are symmetrically disposed in energy with respect to Fermi energy of metal, CT can occur at about half the energy of the intrinsic intermolecular excitations of the adsorbate.

Surface-enhanced resonance Raman scattering

SERS requires that the underlying substrates or adsorbents should be roughened enough to produce nanoscale corrugative surface. The objective of the roughness is to create local features in the surface plasmon that enable enhanced scattering. The nature of this roughness affects the resonant frequencies at which the surface plasmon will scatter light, and for SERS the most effective scattering takes place when excitation frequencies are near the resonant frequency. However, for surface-enhanced resonance Raman scattering (SERRS), the resonance frequencies of the plasmon and the molecular absorption of the analyte have to be considered. The large enhancements in SERS can be further improved by using an analyte having molecular absorption near the resonant frequencies to give strong SERRS signals. The first ever SERRS observation was reported by Van Duyne and his group[9] in 1977. Because of the higher enhancement in SERRS in the range 10^8–10^{14}, several groups, including ours, confirmed the resonance phenomenon and some others changed the detection limit of molecules from an ensemble to the single-molecule level[35,46–49]. Itoh *et al.*[46] reported several observations on correlated plasmon resonance Rayleigh scattering and SERRS using single Ag nanoaggregates.

Surface-enhanced hyper-Raman scattering

The extremely low cross-section of normal hyper-Raman cross-section (~10^{-64} cm^4) can be accessed through a surface-enhanced phenomenon analogous to SERS. Thus, SERS and surface-enhanced hyper-Raman scattering (SEHRS) can appear at comparable signal levels because of strong surface-enhancement factors. Although SEHRS of several dyes adsorbed on the aggregated silver colloids has been reported[50] in the 1980s, its inherent weak intensity hindered the extensive work on SEHRS. Van Duyne and his group reported an estimated surface enhancement factor of 10 from the SEHRS spectra of pyridine adsorbed on the roughened silver electrode[51,52]. Similar observation was also reported by Nie *et al.*[53]. Kneipp *et al.*[54] reported an enhancement factor on the order of 10 comparing the near-infrared (NIR)-SERS enhancement factors of crystal violet on colloidal silver clusters. Several groups, including ours, reported the SEHRS study of molecules adsorbed on different active substrates, including the randomly roughened electrode surfaces, aggregated noble metal colloids, and metal–nanoparticles immobilized-on-smooth-electrodes, to improve the efficiency of SEHRS and to explore its application in chemical, biological and materials sciences[52,55,56]. Itoh *et al.*[56] compared hyper Rayleigh scattering and SEHRS of dye-adsorbed silver nanoparticles using continuous-wave NIR laser. Green emission because of hyper Rayleigh scattering in addition to optical trapping of silver nanoparticles was observed. Strong SEHRS intensity and two-photon excited luminescence were observed on the addition of R6G and NaCl to the samples.

Single molecule surface-enhanced Raman scattering

Detection and molecular characteristics of single molecules by SERS was not possible till the 1990s. The observation of a single molecule and its individual properties and structural transformation can provide useful insights relating to intrinsic characteristics that cannot be studied in an ensemble of molecules due to averaging. Two groups[20,21] independently reported single molecule (SM)-SERS nearly at the same time. It was based on the concept of ultra-low concentration achieved by decreasing the concentration of the analytes adsorbed on a small number of adsorbents. In addition, there are several methodologies reported to obtain SM-SERS[57–60]. Amongst all the techniques, SERS combined with near-field microscopy achieves the best suitable control on the characteristics and spatial localization of a single hotspot producing SM-SERS signals.

Tip-enhanced Raman scattering

SERS from analytes adsorbed on nanostructures is obtained due to the excitation of LSPR. Analogous to this general concept, a single metal nanostructure, i.e. a metallic nanosized needle-like tip, can induce SERS at the tip apex provided that the analytes exist near the apex. Raman scattering enhanced by such a tip is termed as tip-enhanced Raman scattering (TERS). The essential feature is the incident electric field enhancement at the tip apex, thus accessing localized near-fields and avoiding the problem of diffraction of light. It is so attractive that the spatial resolution can be scaled down to few nanometres and the SERS characteristics can be obtained even from single molecules. The development of SERS towards TERS was introduced by combining near-field scanning optical microscopy with the SERS technique. TERS has been accepted as one of the most intriguing developments of SERS[61–65].

Correlated imaging and spectroscopy

Correlated imaging and spectral analysis are two potential ways to understand the influence of SPR on SERS[66–70]. Hossain *et al.*[69] reported correlated SPR and SERS images carried out at the same spatial position using gold nanoaggregates. Good correlation was reported between plasmon excitations and the SERS activity of the same sample. Unlike a dimer or a trimer, localized SPR excitation was observed to be specific to the local structure in nanoscale. Several localized SPR excitations were excited in different parts of the aggregates. Figure 4 *a* and *c* shows SPR and SERS images of gold nanoaggregates respectively. Figure 4 *b* and *d* depicts SPR and SERS spectra

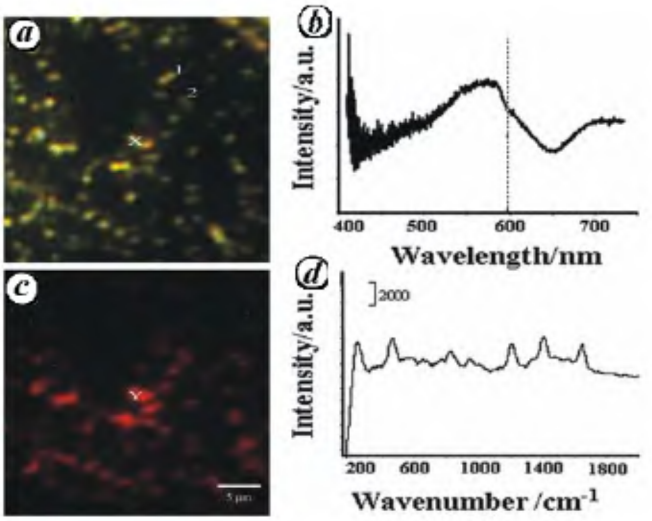

Figure 4. ***a***, SPR image of gold nanoparticle aggregates with 50 nm diameter, indicating intensity variation corresponding to SPR excitations excited on the sample. ***b***, SPR spectrum of the same sample obtained at the marked position 'X' in (***a***), showing a broadened SPR peak centred at 570 nm, in addition to a trail in the longer wavelength region (~700 nm). ***c***, SERS image of CV adsorbed on the same sample indicating good correlation to (***a***). ***d***, SERS spectrum of CV adsorbed on the same sample obtained at the marked position 'Y' in (***c***). The scale bar in (***c***) shows the size of the SPR and SERS images. The dotted vertical line in (***b***) shows the laser excitation position. Reprinted with permission from Hossain *et al.*[69].

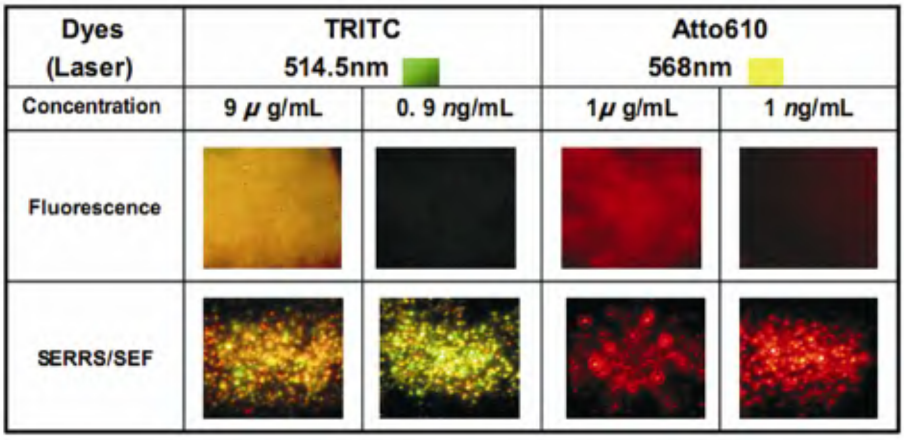

Figure 5. Fluorescence, SERRS and SEF images of TRITC and Attto610 at different concentrations. Reprinted with permission from Han *et al.*[73].

obtained at the 'X' and 'Y' positions in Figure 4 *a* and *c* respectively. A broadened SPR peak centred at 570 nm appears in addition to another peak near the longer wavelength region. The SERS peaks observed here are consistent with those reported so far. In a random aggregate sample, the number of interstitials per micrometre is less and some aggregates are not SERS-active with the laser excitation at 647 nm.

Applications

SERS overcomes the long collection times and high detection limits inherent in normal Raman spectroscopy and makes possible the detection of single cells. SERS is also useful for label-free detection and fluorescence rejection. In addition, NIR photons are not in resonance with molecular transitions and thus avoid photodecomposition of the probed molecule. In the NIR region both silver and gold clusters are used for *in vivo* applications, but gold is more suitable because it is more inert[71,72].

Label-free detection of protein

Several groups, including ours, attempted to detect biomolecules by SERS. Recently, silver nanoparticles conjugated biomolecules have been investigated by Han *et al.*[73] through correlated SERRS and surface enhanced fluorescence (SEF) measurements at the same spatial position. TRITC and Atto610 are used as both Raman and fluorescence reporters through the ligands in the study. Interactions between human IgG and TRITC-anti-human IgG (Fc-specific) and between avidin and Atto610-biotin were detected. Figure 5 shows fluorescence images of two fluorescent molecules after interactions between proteins and target analytes, and their SERRS and SEF images after colloidal silver staining[73]. Note that the SERRS and SEF images of each fluorescent molecule show significant differences with different concentrations of the target analytes. By varying the concentration of fluorescence-labelled target analytes, it was found that at higher concentration or at certain concentrations (9 ng/ml TRITC-anti-human IgG and 1 ng/ml Atto610-biotin), fluorescent images were dominant. This study indicates the potential of SERRS and SEF images in ultrasensitive determination of protein–ligand interactions. Figure 6 shows SERRS and fluorescence spectra of TRITC-labelled immunocomplex (TRITC-antihuman IgG, 0.9 ng/ml) and Atto610-labeled biotin/avidin complex (Atto610-biotin, 0.1 ng/ml)[73]. Strong enhanced Raman scattering and fluorescence were obtained.

Ultrafast detection

Spectroscopy of single haemoglobin molecules, glucose detection and cancer gene detection are few examples of ultrafast detection by the SERS technique[74–77]. A new trend in biochip technology for label free detection of pathogens and their toxins has also been introduced recently[59]. Unlike fluorescence, SERS is not limited by the need to label and photobleaching, and hence provides detailed chemical information about molecules even in a complex environment. Fast acquisition time and higher enhancement factor have made the SERS technique irreplaceable in detecting molecules mixed with complex environment.

Bioimaging and living cells

SERS appears to be an informative method for the study of living cells both in intracellular and extracellular measurements. Eliasson *et al.*[3] identified biomolecules or intracellular components independently in single cells by SERS measurements on gold-incorporated lymphocyte living cell. Distinguished rhodamine signal from the

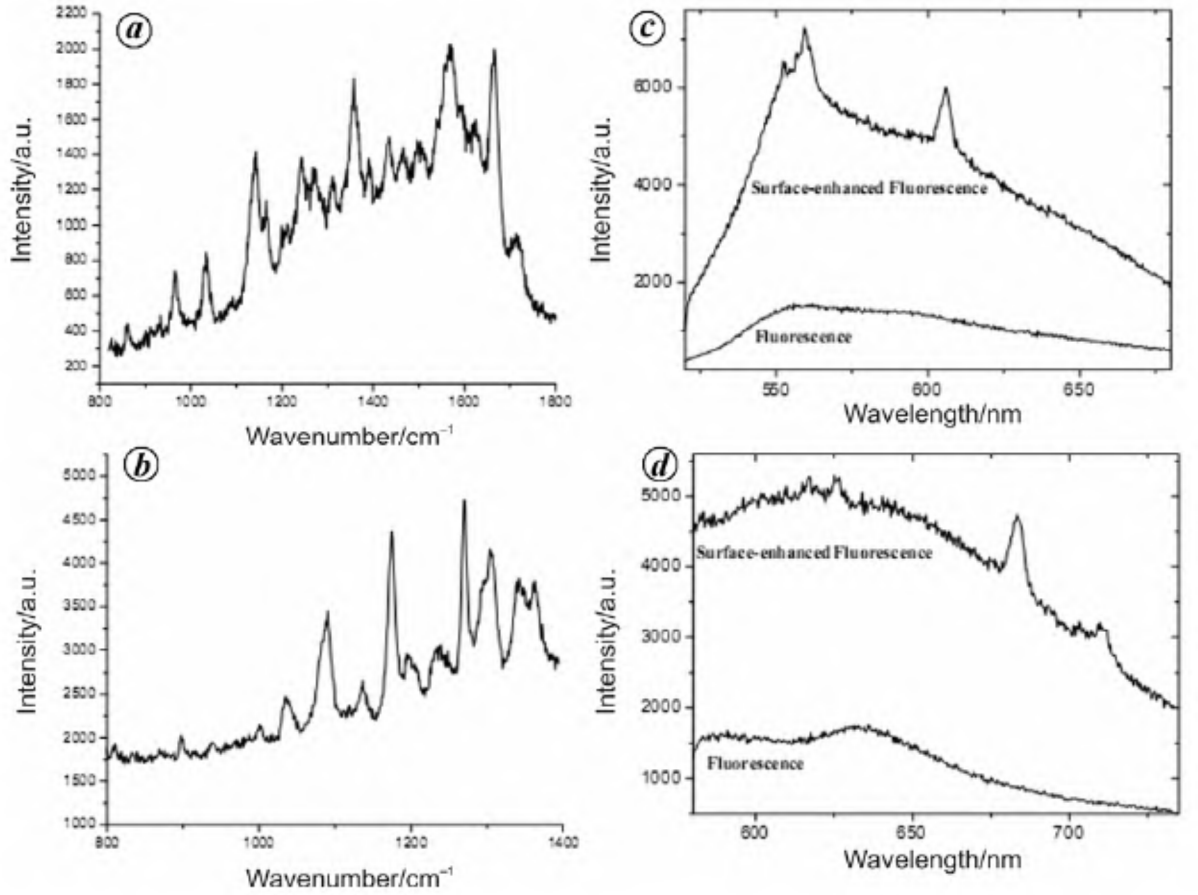

Figure 6. ***a***, SERRS spectra of TRITC-labelled immunocomplex with 514.5 nm excitation. ***b***, SERRS spectra of Atto610-labelled biotin/avidin complex with 568 nm laser excitation. ***c***, Fluorescence and SEF spectra of TRITC-labelled immunecomplex (0.9 ng/ml TRITC-anti-human IgG) with 514.5 nm laser excitation. ***d***, Fluorescence and SEF spectra of Atto610-labelled biotin/avidin complex (0.1 ng/ml Atto610-biotin) with 568 nm excitation. Reprinted with permission from Han *et al.*[73].

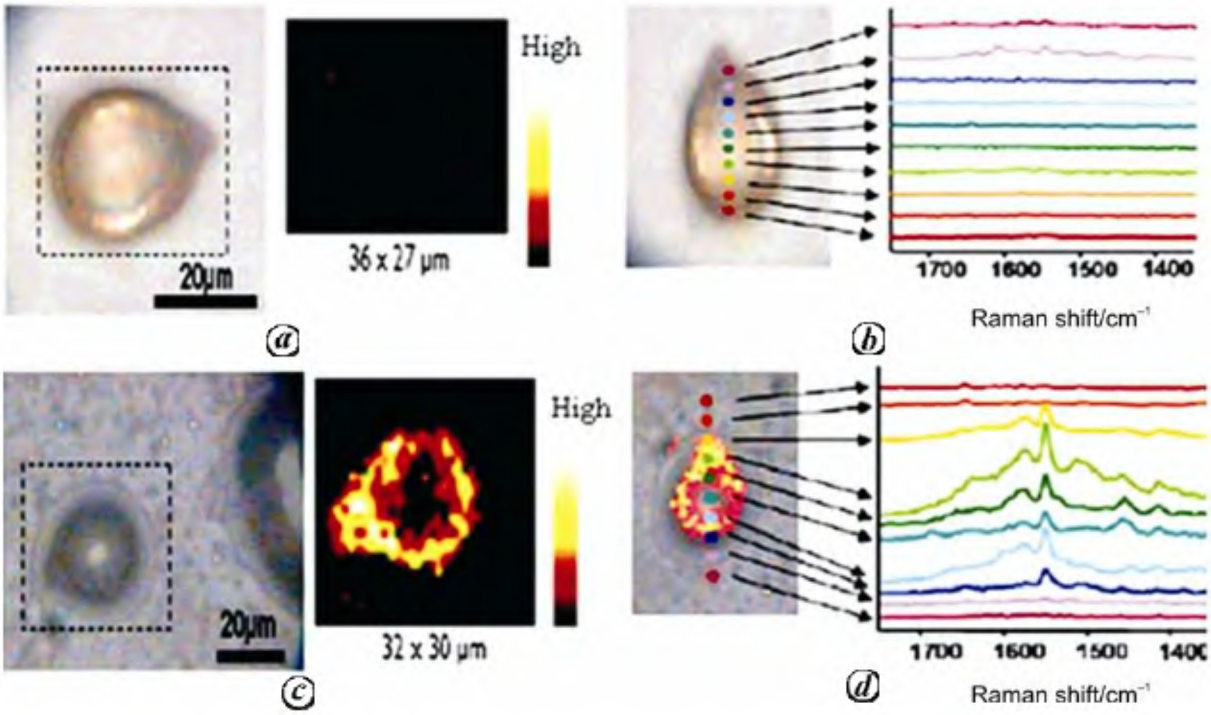

Figure 7. ***a***, Normal cell dark field image and SERS spectroscopy image. ***b***, Raman measurements. ***c***, Single cancer cell: bright field image (left), SERS image (right). ***d***, Bright-field image and SERS mapping for single cancer cell. Reprinted with permission from Lee *et al.*[79].

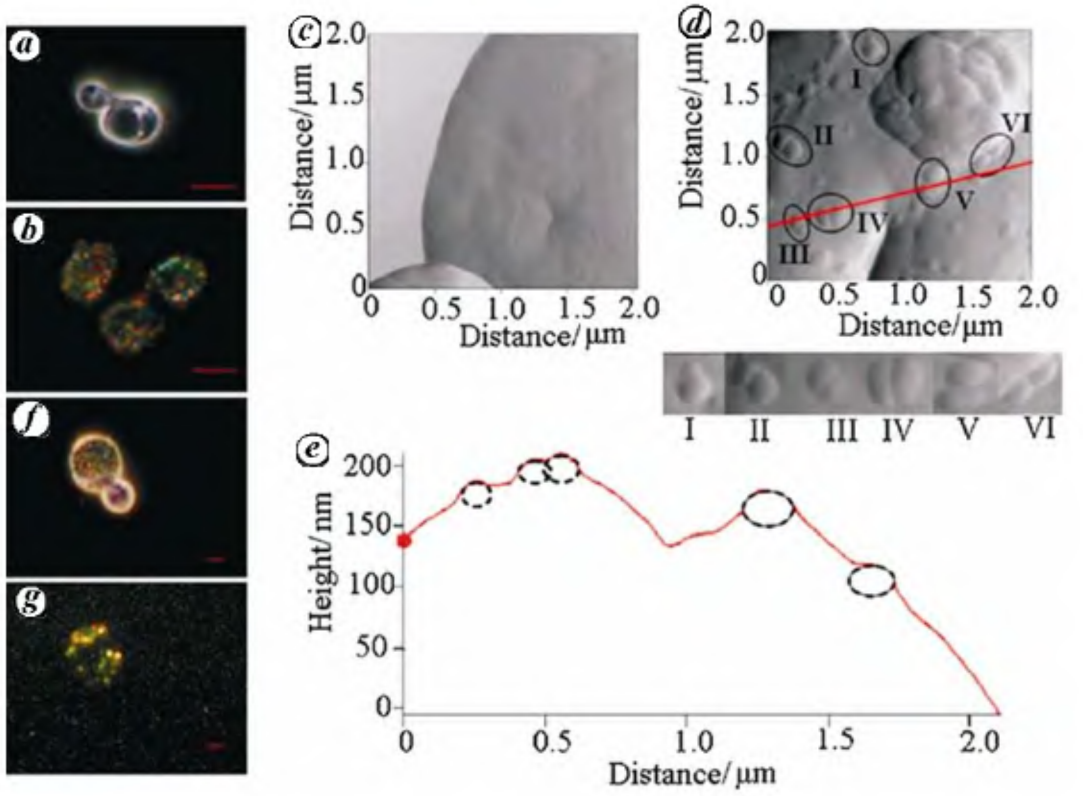

Figure 8. ***a***, Dark field image of a yeast cell. ***b***, Dark field image of Ag adsorbed on yeast cell surfaces (scale 1 μm). ***c***, AFM images of a yeast cell. ***d***, AFM image of Ag adsorbed yeast cell. ***e***, Height trace along the line drawn therein. ***f***, Ag nanoaggregates on a yeast cell surface. ***g***, The corresponding SERS image (scale 1 μm). Reprinted with permission from Sujith *et al.*[80].

combined intercellular components of lymphocyte single living cell was successfully detected. On the other hand, silver colloidal aggregates have been incubated with breast cancer-resistant cells to elucidate the affinity amongst the cellular components. SERS is not only of interest as a method for ultrasensitive detection and structural characterization of biomolecules, but it has been also applied to study processes of living cells. Breuzard *et al.*[4] applied SERS to study the adsorption of mitoxantrone on the plasma membrane of sensitive (HCT-116 S) or BCRP/MXR-type resistant (HCT-116 R) cells.

Kneipp *et al.*[78] proposed a sensitive optical probe based on the SERS spectroscopic signature of dye indocyanine green ICG on gold nanoparticles. In addition to its own detection, the *in vivo* compatible ICG-gold nanoprobe also delivers local molecular structural information about its biological environment. This may become important for understanding cellular processes. The spectra provide clear evidence for vibrations originating from the DNA backbone and of C-N and ring stretching modes from DNA and RNA. SERS has recently been successfully applied to differentiate cancerous cells. For example, to obtain a highly sensitive cellular image of living normal HEK293 cells and HEK293 cells expressing PLCγ1 using the SERS technique, functional nanoprobes based on Au/Ag core-shell nanoparticles, conjugated with monoclonal antibodies, were used by Lee *et al.*[79]. PLCγ1 is a protein whose abnormal expression may be associated with tumour development. A schematic illustration of silver-coated gold nanoprobes with R6G for the SERS imaging of cancer cells is given in Figure 7.

Sujith *et al.*[80] recently attempted to study the cell-wall biochemistry of living single yeast by SERS. Figure 8 *a* and *b* shows dark field images of living yeast cells without and with Ag nanoparticles respectively. This correspondence is evident from AFM images of a yeast cell surface (Figure 8 *c*) and a yeast cell surface adsorbed with Ag nanoparticles (Figure 8 *d*). Figure 8 *f* and *g* shows the dark field and corresponding SERS image of Ag nanoparticles adsorbed on the cell wall respectively.

Conclusion

The academic understanding of SERS has promoted many practical applications, such as photonic materials, heterogenous catalysis, chemosensors, biosensors, optical traps and tweezers, near-field optical microscopy, and other surface-enhanced spectroscopies. Though there are still unanswered questions, the advancement of knowledge regarding Raman effect and SERS in the last 80

years has provided a solid foundation for continued research and development in the 21st century. The understanding and development of SERS could be substantially advanced by the steady progress of nanotechnology. Thus SERS and nanotechnology would expect to support each other in the near future.

It is noteworthy that the outcomes reported herein are a small part of several studies on SERS in different laboratories. There are still several to be investigated, including the nature of the photon–electron interaction process, the excitation and relaxation behaviour of LSPR, quenching effect of confined EM fields due to secondary roughness of the constituent nanoparticles, hybridization and percolation of highly localized energy, etc. We are looking forward to the dedicated scientists and mentors for rigorous and evidential support in the SERS world. Thanks to C. V. Raman for initiating such a useful and comprehensive analytical tool for modern science and nanotechnology.

1. Chalmers, J. M. and Griffiths, R. R., *Handbook of Vibrational Spectroscopy*, John Wiley, Chichester, 2002.
2. Bulte, J. W. M. and Modo, M. M. J., *Nanoparticles in Biomedical Imaging: Emerging Technologies and Applications*, Springer Science & Business Media, New York, 2008.
3. Eliasson, C., Loren, A., Engelbrektsson, J., Josefson, M., Abrahamsson, J. and Abrahamsson, K., Surface-enhanced Raman scattering imaging of single living lymphocytes with multivariate evaluation. *Spectrochim. Acta, Part A*, 2005, **61**, 755–760.
4. Breuzard, G., Angiboust, J. F., Jeannesson, P., Manfait, M. and Millot, J. M., Surface-enhanced Raman scattering reveals adsorption of mitoxantrone on plasma membrane of living cells. *Biochem. Biophys. Res. Commun.*, 2004, **320**, 615–621.
5. Nei, S. and Emory, S. R., Probing single molecules and single nanoparticles by surface-enhanced Raman scattering. *Science*, 1997, **275**, 1102–1106.
6. Dou, X., Jung, Y. M., Cao, Z. and Ozaki, Y., Surface-enhanced Raman scattering of biological molecules on metal colloid II: effects of aggregation of gold colloid and comparison of effects of pH of glycine solutions between gold and silver colloids. *Appl. Spectrosc.*, 1999, **53**, 1440–1447.
7. Yonzon, C. R., Haynes, C. L., Zhang, X., Walsh, J. T. and Van Duyne, R. P., A glucose biosensor based on surface-enhanced Raman scattering: improved partition layer, temperature stability, reversibility and resistance to serum protein interference. *Anal. Chem.*, 2004, **76**, 78–85.
8. Fleischmann, M., Hendra, P. J. and McQuillan, A. J., Raman spectra of pyridine adsorbed at a silver electrode. *Chem. Phys. Lett.*, 1974, **26**, 163–166.
9. Jeanmaire, D. L. and Van Duyne, R. P., Surface Raman spectroelectrochemistry: Part I. Heterocyclic, aromatic, and aliphatic amines adsorbed on the anodized silver electrode. *J. Electroanal. Chem.*, 1977, **84**, 1–20.
10. Albrecht, M. G. and Creighton, J. A., Anomalously intense Raman spectra of pyridine at a silver electrode. *J. Am. Chem. Soc.*, 1977, **99**, 5215–5217.
11. Tian, Z. Q. and Ren, B., Adsorption and reaction at electrochemical interfaces as probed by surface-enhanced Raman spectroscopy. *Annu. Rev. Phys. Chem.*, 2004, **55**, 197–229.
12. Moore, C. B., *Chemical and Biochemical Applications of Lasers*, Academic Press, New York, 1979.
13. Kneipp, K., Kneipp, H., Itzkan, I., Dasari, R. R. and Feld, M. S., Ultrasensitive chemical analysis by Raman spectroscopy. *Chem. Rev.*, 1999, **99**, 2957–2975.
14. Campion, A. and Kambhampati, P., Surface-enhanced Raman scattering. *Chem. Soc. Rev.*, 1998, **27**, 241–250.
15. Haynes, C. L., McFarland, A. D. and Van Duyne, R. P., Surface-enhanced Raman scattering. *Anal. Chem.*, 2005, **77**, 338A–346A.
16. Moskovits, M., Surface-enhanced Raman scattering. *Rev. Mod. Phys.*, 1985, **57**, 783–823.
17. Kneipp, K., Kneipp, H., Itzkan, I., Dasari, R. R. and Feld, M. S., Surface enhanced Raman scattering and biophysics. *J. Phys.: Condens. Matter*, 2002, **14**, R597–R624.
18. Moskovits, M., Surface roughness and the enhanced intensity of Raman scattering by molecules adsorbed on metals. *J. Chem. Phys.*, 1978, **69**, 4159–4161.
19. Otto, A., Timper, J., Billmann, J., Kovacs, G. and Pockrand, I., Surface roughness induced electronic Raman scattering. *Surf. Sci.*, 1980, **92**, L55–L57.
20. Kneipp, K., Wang, Y., Kneipp, H., Perelman, L. T., Itzkan, I., Dasari, R. R. and Feld, M. S., Single molecule detection using surface-enhanced Raman scattering (SERS). *Phys. Rev. Lett.*, 1997, **78**, 1667–1670.
21. Nie, S. and Emory, S. R., Probing single molecules and single nanoparticles by surface-enhanced Raman scattering. *Science*, 1997, **275**, 1102–1106.
22. Zhang, P., Haslett, T. L., Douketis, C. and Moskovits, M., Mode localization in self-affine fractal interfaces observed by near-field microscopy. *Phys. Rev. B*, 1998, **57**, 15513–15518.
23. Xu, H., Aizpurua, J., Käll, M. and Apell, P., Electromagnetic contributions to single-molecule sensitivity in surface-enhanced Raman scattering. *Phys. Rev. E*, 2000, **62**, 4318–4324.
24. Nalwa, H. S., *Encyclopedia of Nanoscience & Nanotechnology*, American Scientific Publishers, USA, 2004.
25. Raether, H., *Surface Plasmons*, Springer-Verlag, New York, 1986, p. 26.
26. Brongersma, M. L. and Kik, P. G., *Surface Plasmon Nanophotonics*, Springer, Dordrecht, 2007.
27. Kneipp, K., Moskovit, M. and Kneipp, H., *Surface-enhanced Raman Scattering: Physics and Applications*, Springer-Verlag, Berlin, 2006.
28. Haes, J. and Van Duyne, R. P., Preliminary studies and potential applications of localized surface plasmon resonance spectroscopy in medical diagnostics. *Expert Rev. Mol. Diagn.*, 2004, **4**, 527–537.
29. Altewischer, E., Van Exter, M. P. and Woedman, J. P., Plasmon-assisted transmission of entangled photons. *Nature*, 2002, **418**, 304–306.
30. Elghanian, R., Storhoff, J. J., Mucic, R. C., Letsinger, R. L. and Mirkin, C. A., Selective colorimetric detection of polynucleotides based on the distance dependent optical properties of gold nanoparticles. *Science*, 1997, **277**, 1078–1081.
31. Li, K., Stockman, M. I. and Bergman, D. J., Self-similar chain of metal nanospheres as an efficient nanolens. *Phys. Rev. Lett.*, 2003, **91**, 227402-1–227402-4.
32. Hossain, M. K., Shimada, T., Kitajima, M., Imura, K. and Okamoto, H., Near field Raman imaging and electromagnetic field confinement in the self-assembled monolayer array of gold nanoparticles. *Langmuir*, 2008, **24**, 9241–9244.
33. Maier, S. A. and Atwater, H. A., Plasmonics: localization and guiding of electromagnetic energy in metal/dielectric structures. *J. Appl. Phys.*, 2005, **98**, 011101-1–011101-10.
34. Mock, J. J., Smith, D. R. and Schultz, S., Local refractive index dependence of plasmon resonance spectra from individual nanoparticles. *Nano Lett.*, 2003, **3**, 485–491.
35. Itoh, T., Biju, V., Ishikawa, M., Kikkawa, Y., Hashimoto, K., Ikehata, A. and Ozaki, Y., Surface-enhanced resonance Raman scat-

tering and background light emission coupled with plasmon of single Ag nanoaggregates. *J. Chem. Phys.*, 2006, **124**, 134708–134713.
36. Pettinger, B., Light scattering by adsorbates at Ag particles: quantum-mechanical approach for energy transfer induced interfacial optical processes involving surface plasmons, multipoles, and electron-hole pairs. *J. Chem. Phys.*, 1986, **85**, 7442–7451.
37. Itoh, T., Yoshida, K., Biju, V., Kikkawa, Y., Ishikawa, M. and Ozaki, Y., Second enhancement in surface-enhanced resonance Raman scattering revealed by an analysis of anti-Stokes and Stokes Raman spectra. *Phys. Rev. B*, 2007, **76**, 085405–085410.
38. Michaels, A. M., Nirmal, M. and Brus, L. E., Surface-enhanced Raman spectroscopy of individual rhodamine 6G molecules on large Ag nanocrystals. *J. Am. Chem. Soc.*, 1999, **121**, 9932–9939.
39. Etchegoin, P. *et al.*, A novel amplification mechanism for surface enhanced Raman scattering. *Chem. Phys. Lett.*, 2002, **366**, 115–121.
40. Otto, A., Mrozek, I., Grabhorn, H. and Akemann, W., Surface-enhanced Raman scattering. *J. Phys.: Condens Matter*, 1992, **4**, 1143–1212.
41. Otto, A., On the electronic contribution to single molecule surface enhanced Raman spectroscopy. *Indian J. Phys.*, 2003, **77B**, 63–73.
42. Persson, B. N. J., On the theory of surface-enhanced Raman scattering. *Chem. Phys. Lett.*, 1981, **82**, 561–565.
43. Arenas, J. F., Woolley, M. S., Tocon, I. L., Otero, J. C. and Marcos, J. I., Complete analysis of the surface-enhanced Raman scattering of pyrazine on the silver electrode on the basis of a resonant charge transfer mechanism involving three states. *J. Chem. Phys.*, 2000, **112**, 7669–7983.
44. Billmann, J., Kovakcs, G. and Otto, A., Raman spectroscopy of carbon monoxide adsorbed on silver island films. *Surf. Sci.*, 1990, **238**, 192–198.
45. Otto, A., Surface-enhanced Raman scattering of adsorbates. *J. Raman Spectrosc.*, 1991, **22**, 743–752.
46. Itoh, T., Kikkawa, Y., Yoshida, K., Hashimoto, K., Biju, V., Ishikawa, M. and Ozaki, Y., Correlated measurements of plasmon resonance Rayleigh scattering and surface-enhanced resonance Raman scattering using a dark-field microspectroscopic system, *J. Photochem. Photobiol. A*, 2006, **183**, 322–328.
47. Hildebrandt, P. and Stockburger, M., Surface-enhanced resonance Raman spectroscopy of rhodamine 6G adsorbed on colloidal silver. *J. Phys. Chem.*, 1984, **88**, 5935–5944.
48. Bizzarri, A. R. and Cannistraro, S., Surface-enhanced resonance Raman spectroscopy signals from single myoglobin molecules. *Appl. Spectrosc.*, 2002, **56**, 1531–1537.
49. Tolaieb, B., Constantino, C. J. L. and Aroca, R. F., Surface-enhanced resonance Raman scattering as an analytical tool for single molecule detection. *Analyst*, 2004, **129**, 337–341.
50. Murphy, D. V., Von Raben, K. U., Chang, R. K. and Dorain, P. B., Surface enhanced hyper-Raman scattering from SO32-adsorbed on Ag powder. *Chem. Phys. Lett.*, 1982, **85**, 43–47.
51. Golab, J. T., Sprague, J. R., Carron, K. T., Schatz, G. C. and Van Duyne, R. P., A surface enhanced hyper-Raman scattering study of pyridine adsorbed onto silver: experiment and theory. *J. Chem. Phys.*, 1988, **88**, 7942–7951.
52. Yang, W. H., Hulteen, J., Schatz, G. C. and Van Duyne, R. P., A surface enhanced hyper-Raman and surface-enhanced Raman scattering study of trans1,2-*bis*(4-pyridyl)ethylene adsorbed onto silver film over nanosphere electrodes. Vibrational assignments: experiment and theory. *J. Chem. Phys.*, 1996, **104**, 4313–4323.
53. Nie, S. M., Lipscomb, L. A. and Yu, N. T., Surface-enhanced hyper-Raman spectroscopy. *Appl. Spectrosc. Rev.*, 1991, **26**, 203–276.
54. Kneipp, H., Kneipp, K. and Seifert, F., Surface-enhanced hyper-Raman scattering (SEHRS) and surface-enhanced Raman scattering (SERS) by means of mode-locked Ti : sapphire laser excitation. *Chem. Phys. Lett.*, 1993, **212**, 374–378.
55. Kneipp, K., Kneipp, H., Itzkan, I., Dasari, R. R., Feld, M. S. and Dresselhauset, M. S., Nonlinear Raman probe of single molecules attached to colloidal silver and gold clusters. *Top. Appl. Phys.*, 2002, **82**, 227–249.
56. Itoh, T., Ozaki, Y., Yoshikawa, H., Ihama, T. and Masuhara, H., Hyper Rayleigh scattering and hyper Raman scattering of dye-adsorbed silver nanoparticles induced by focused continuous-wave near-infrared laser. *Appl. Phys. Lett.*, 2006, **88**, 084102-1–084102-3.
57. Le Ru, E. C., Meyer, M. and Etchegoin, P. G., Proof of single-molecule sensitivity in surface-enhanced Raman scattering (SERS) by means of a two analyte technique. *J. Phys. Chem. B*, 2006, **110**, 1944–1948.
58. Constantino, C. J. L., Lemma, T., Antunes, P. A. and Aroca, R. F., Single molecule detection using surface-enhanced resonance Raman scattering and Langmuir–Blodgett monolayers. *Anal. Chem.*, 2001, **73**, 3674–3678.
59. Goulet, P. J. G. and Aroca, R. F., Distinguishing individual vibrational fingerprints: single-molecule surface-enhanced resonance Raman scattering from one-to-one binary mixtures in Langmuir–Blodgett monolayers. *Anal. Chem.*, 2007, **29**, 2728–2734.
60. Etchegoin, P. G., Meyer, M., Blackie, E. and Le Ru, E. C., Statistics of single molecule surface-enhanced Raman scattering signals: fluctuation analysis with multiple analyte techniques. *Anal. Chem.*, 2007, **79**, 8411–8415.
61. Hayazawa, N. Inouye, Sekkat, Z. and Kawata, S., Near-field Raman imaging of organic molecules by an apertureless metallic probe scanning optical microscope. *J. Chem. Phys.*, 2002, **117**, 1296–1301.
62. Anderson, M. S., Locally enhanced Raman spectroscopy with an atomic force microscope. *Appl. Phys. Lett.*, 2000, **76**, 3130–3132.
63. Hartschuh, A., Sanchez, E. J., Xie, X. S. and Novotny, L., High-resolution near field Raman microscopy of single-walled carbon nanotubes. *Phys. Rev. Lett.*, 2003, **90**, 95503–95506.
64. Micic, M., Klymyshyn, N., Suh, Y. D. and Lu, H. P., Finite element method simulation of the field distribution for AFM tip-enhanced surface-enhanced Raman scanning microscopy. *J. Phys. Chem. B*, 2003, **107**, 1574–1584.
65. Pettinger, B., Picardi, G., Schuster, R. and Ertl, G., Surface-enhanced and STM tip-enhanced Raman spectroscopy of CN-ions at gold surfaces. *J. Electroanal. Chem.*, 2003, **554–555**, 293–299.
66. Zhang, P., Smith, S., Rumbles, G. and Himmel, M. E., Direct imaging of surface enhanced Raman scattering in the near field. *Langmuir*, 2005, **21**, 520–523.
67. Hossain, M. K., Shimada, T., Kitajima, M., Imura, K. and Okamoto, H., Raman and near-field spectroscopic study on localized surface plasmon excitation from the 2D nanostructure of gold nanoparticles. *J. Microsc.*, 2008, **229**, 327–330.
68. Shimada, T., Imura, K., Hossain, M. K., Kitajima, M. and Okamoto, H., Near field study on correlation of localized electric field and nanostructures in monolayer assembly of gold nanoparticles. *J. Phys. Chem. C*, 2008, **112**, 4033–4035.
69. Hossain, M. K., Kitahama, Y., Huang, G. G., Kaneko, T. and Ozaki, Y., SPR and SERS characteristics of gold nanoaggregates with different morphologies. *Appl. Phys. B*, 2008, **93**, 165–170.
70. Imura, K., Okamoto, Hossain, M. K. and Kitajima, M., Visualization of localized intense optical fields in single gold-nanoparticle assemblies and ultrasensitive Raman active sites. *Nano Lett.*, 2006, **6**, 2173–2176.
71. Chourpa, I., Lei, F. H., Dubois, P., Manfaita, M. and Sockalingum, G. D., Intracellular applications of analytical SERS spectro-

scopy and multispectral imaging. *Chem. Soc. Rev.*, 2008, **37**, 993–1000.

72. Kneipp, K. *et al.*, Surface-enhanced Raman spectroscopy in single living cells using gold nanoparticles. *Appl. Spectrosc.*, 2002, **56**, 150–154.
73. Han, X. X., Kitahama, Y., Tanaka, Y., Guo, J., Xu, W. Q., Zhao, B. and Ozaki, Y., Simplified protocol for detection of protein–ligand interactions via surface enhanced resonance Raman scattering and surface-enhanced fluorescence. *Anal. Chem.*, 2008, **80**, 6567–6572.
74. Xu, H., Bjerneld, E. J., Kall, M. and Borjesson, L., Spectroscopy of single hemoglobin molecules by surface-enhanced Raman scattering. *Phys. Rev. Lett.*, 1999, **83**, 4357–4360.
75. Vo-Dinh, T., Allain, L. R. and Stokes, D. L., Cancer gene detection using surface enhanced Raman scattering (SERS). *J. Raman Spectrosc.*, 2002, **33**, 511–516.
76. Cao, Y. C., Jin, R. and Mirkin, C. A., Nanoparticles with Raman spectroscopy fingerprint for DNA and RNA detection. *Science*, 2002, **297**, 1536–1540.
77. Grow, A. E., Wood, L. L., Claycomb, J. L. and Thompson, P. A., New biochip technology for label free detection of pathogens and their toxins. *J. Microbiol. Methods*, 2003, **53**, 221–233.
78. Kneipp, J., Kneipp, H., Rice, W. L. and Kneipp, K., Optical probes for biological applications based on surface-enhanced Raman scattering from indocyanine green on gold nanoparticles. *Anal. Chem.*, 2005, **77**, 2381–2385.
79. Lee, S. *et al.*, Biological imaging of HEK293 cells expressing PLCγ1 using surface-enhanced Raman microscopy. *Anal. Chem.*, 2007, **79**, 916–922.
80. Sujith, A., Itoh, T., Abe, H., Anas, A., Yoshida, K., Biju, V. and Ishikawa, M., Surface enhanced Raman scattering analyses of individual silver nanoaggregates on living single yeast cell wall. *Appl. Phys. Lett.*, 2008, **92**, 103901–103903.